Micro-SPECT/CT with ^{111}In-DTPA-Pertuzumab Sensitively Detects Trastuzumab-Mediated *HER2* Downregulation and Tumor Response in Athymic Mice Bearing MDA-MB-361 Human Breast Cancer Xenografts

Kristin McLarty[1], Bart Cornelissen[1], Zhongli Cai[1,2], Deborah A. Scollard[1], Danny L. Costantini[1], Susan J. Done[3,4], and Raymond M. Reilly[1,2,5]

[1]Department of Pharmaceutical Sciences, University of Toronto, Toronto, Ontario, Canada; [2]Toronto General Research Institute, University Health Network, Toronto, Ontario, Canada; [3]Department of Medical Biophysics and Department of Laboratory Medicine and Pathobiology, University of Toronto, Toronto, Ontario, Canada; [4]Ontario Cancer Institute and Department of Pathology, University Health Network, Toronto, Ontario, Canada; and [5]Department of Medical Imaging, University of Toronto, Toronto, Ontario, Canada

Pertuzumab is a *HER2* dimerization inhibitor that binds to an epitope unique from that of trastuzumab. Our objective was to determine whether SPECT with ^{111}In-diethylenetriaminepenta-acetic acid–pertuzumab (^{111}In-DTPA-pertuzumab) could sensitively detect an early molecular response to trastuzumab manifested by *HER2* downregulation and a later tumor response revealed by a decreased number of *HER2*-positive viable tumor cells. **Methods:** Changes in *HER2* density in SKBr-3 and MDA-MB-361 BC cells exposed to trastuzumab (14 μg/mL) in vitro were measured by saturation binding assays using ^{111}In-DTPA-pertuzumab and by confocal immunofluorescence microscopy and flow cytometry with fluorescein isothiocyanate–labeled *HER2/neu* antibodies. Imaging of *HER2* downregulation was studied in vivo in athymic mice with subcutaneous MDA-MB-361 tumors treated for 3 d with trastuzumab (4 mg/kg) or nonspecific human IgG (hIgG) or phosphate-buffered saline (PBS). Imaging of tumor response to trastuzumab was studied in mice bearing subcutaneous MDA-MB-361 xenografts treated with trastuzumab (4 mg/kg), followed by weekly doses of nonspecific hIgG or rituximab or PBS (2 mg/kg). Mice were imaged on a micro-SPECT/CT system at 72 h after injection of ^{111}In-DTPA-pertuzumab. Tumor and normal-tissue biodistribution was determined. **Results:** ^{111}In-DTPA-pertuzumab saturation binding to SKBr-3 and MDA-MB-361 cells was significantly decreased at 72 h after exposure in vitro to trastuzumab (14 μg/mL), compared with untreated controls (62% ± 2%, $P < 0.0001$; 32% ± 9%, $P < 0.0002$, respectively). After 3 d of trastuzumab, in vivo tumor uptake of ^{111}In-DTPA-pertuzumab decreased 2-fold in trastuzumab- versus PBS-treated mice (13.5 ± 2.6 percentage injected dose per gram [%ID/g] vs. 28.5 ± 9.1 %ID/g, respectively; $P < 0.05$). There was also a 2-fold decreased tumor uptake in trastuzumab- versus PBS-treated mice by image volume-of-interest analysis ($P = 0.05$), suggesting trastuzumab-mediated *HER2* downregulation. After 3 wk of trastuzumab, tumor uptake of ^{111}In-DTPA-pertuzumab decreased 4.5-fold, compared with PBS-treated mice (7.6 ± 0.4 vs. 34.6 ± 9.9 %ID/g, respectively; $P < 0.001$); this decrease was associated with an almost-completed eradication of *HER2*-positive tumor cells determined immunohistochemically. **Conclusion:** ^{111}In-DTPA-pertuzumab sensitively imaged *HER2* downregulation after 3 d of treatment with trastuzumab and detected a reduction in viable *HER2*-positive tumor cells after 3 wk of therapy in MDA-MB-361 human breast cancer xenografts.

Key Words: *HER2*; trastuzumab; molecular imaging; tumor response; pertuzumab

Molecular imaging is a powerful new tool that has great potential for aiding in the optimal use of novel targeted cancer therapies by revealing the expression of target receptors in situ on lesions throughout the body; probing downstream treatment-induced molecular events, thus providing early mechanistic evidence of tumor response; and monitoring the prior existence or emergence of resistance pathways implicated in treatment failure (*1*). Trastuzumab (Herceptin; Roche Pharmaceuticals) is a humanized IgG₁ monoclonal antibody (mAb) approved for the treatment of early and advanced breast cancer (BC) which overexpresses the *HER2* transmembrane tyrosine kinase (*2,3*). *HER2* positivity is evaluated in a primary BC biopsy by immunohistochemical staining for *HER2* protein or probing *HER2* gene amplification by fluorescence in situ hybridization (*4*). Despite recent revisions to the standards for *HER2* testing (*4*), only about 1 in 2

patients with metastatic *HER2*-amplified tumors benefit from trastuzumab combined with paclitaxel or anthracyclines (*5*). Novel approaches that more sensitively and accurately predict or monitor response to trastuzumab are needed.

HER2 expression can be imaged in situ in tumors by SPECT or PET using radiolabeled mAbs, antibody fragments (e.g., Fab or F(ab′)$_2$), engineered antibody forms (e.g., minibodies, diabodies, or scFvs), or Affibodies (Affibody AB) (*6–12*).

Response or resistance to trastuzumab is manifested at the molecular level, yet few studies have attempted to probe these pivotal early downstream molecular events. The routes through which trastuzumab exerts its antitumor effects are complex and multifactorial (*13*). Nonetheless, one putative downstream mechanism of action is to promote *HER2* downregulation, thereby diminishing receptor-activated mitogenic signaling (*14*). In this study, we investigated ^{111}In-diethylenetriaminepentaacetic acid (DTPA)–pertuzumab (Omnitarg; Genentech Inc.) as a sensitive probe of trastuzumab-mediated *HER2* downregulation in human BC xenografts in athymic mice and their response to treatment with the drug. Our hypothesis was that trastuzumab-mediated downregulation of *HER2* would result in a decreased tumor imaging signal for ^{111}In-DTPA-pertuzumab, which would not be affected by the binding of trastuzumab to *HER2* (i.e., receptor blocking) because of the unique epitopes of these 2 antibodies. We further hypothesized that the response to trastuzumab would be manifested over a longer time by a decreased imaging signal due to eradication of viable *HER2*-overexpressing tumor cells.

MATERIALS AND METHODS

BC Cells

MDA-MB-361, MDA-MB-231, and SKBr-3 cells were purchased from the American Type Culture Collection. MDA-MB-361 and MDA-MB-231 were cultured in Leibovitz L15 medium (Sigma-Aldrich) supplemented with 20% and 10% fetal bovine serum (Invitrogen), respectively, under a 100% air atmosphere at 37°C. SKBr-3 cells were cultured in RPMI 1640 medium supplemented with 10% fetal bovine serum under a 5% CO_2 atmosphere at 37°C.

^{111}In-DTPA-Pertuzumab

Pertuzumab was derivatized with a 4-fold molar excess of DTPA dianhydride (Sigma-Aldrich). Briefly, a solution of DTPA (2.7 mmol/L) in anhydrous dimethyl sulfoxide was reacted with 34 μL of pertuzumab (15 μg/μL in 50 mM $NaHCO_3$ buffer, pH 8.0) for 1 h at room temperature (RT). Excess DTPA was removed by ultrafiltration on a Microcon YM-50 device (Millipore), with an excess of 1 mol/L sodium acetate buffer, pH 6.0. DTPA substitution was measured as previously reported (*7*). Purified DTPA-pertuzumab was labeled with ^{111}In by incubation with ^{111}In-acetate for 1 h at RT. The reaction mixture was purified on a Sephadex G-50 minicolumn (Sigma-Aldrich). The final radiochemical purity (RCP) was measured by instant thin-layer silica gel chromatography (Pall Life Sciences) developed in sodium citrate (100 mmol/L, pH 5.0) (*12*). The RCP was confirmed by size-exclusion high-performance liquid chromatography (SE-HPLC) as previously reported (*7*). The

immunoreactivity of ^{111}In-DTPA-pertuzumab was determined by measuring its dissociation constant (K_d) and receptor density (B_{max}) in direct saturation binding assays using SKBr-3 cells (*7*).

Competition for HER2 Binding on BC Cells

Competition for binding of ^{111}In-DTPA-pertuzumab to *HER2* in the presence of trastuzumab was studied by seeding 8×10^4 SKBr-3 or 1×10^5 MDA-MB-361 cells in 24-well plates (Sarstedt) and culturing overnight. The culture medium was removed and the adherent cells rinsed with ice-cold phosphate-buffered saline (PBS), pH 7.0. Cells were then incubated with ^{111}In-DTPA-pertuzumab (500 pmol/L) in the presence of increasing concentrations (0–0.5 μmol/L) of trastuzumab in 400 μL of serum-free medium for 3 h at 4°C. The medium was removed, and the cells were rinsed and finally solubilized in 135 μL of NaOH (100 mmol/L). Solubilized cells were transferred to γ-counting tubes and the wells rinsed twice with PBS, and these rinses were combined with those previously removed. The cell-bound radioactivity was measured in a γ-counter (Wizard 3; PerkinElmer) and plotted as the amount of ^{111}In-DTPA-pertuzumab (nanomole-bound) versus the concentration of trastuzumab (nanomoles per liter) using software (Prism, version 4.0; GraphPad Inc.). The assays were performed in duplicate and repeated in 3 separate experiments.

Effect of Trastuzumab on Binding of ^{111}In-DTPA-Pertuzumab In Vitro

Approximately 5×10^4 SKBr-3 or 8×10^4 MDA-MB-361 cells were seeded in 24-well plates and cultured overnight. The medium was removed and the cells incubated at 37°C for 24, 48, or 72 h with trastuzumab (0–56 μg/mL) in 500 μL of fresh medium. The medium was again removed and the cells rinsed in cold PBS. The cells were then incubated with increasing concentrations (0–120 nmol/L) of ^{111}In-DTPA-pertuzumab in serum-free medium for 3 h at 4°C. The medium containing the unbound radioactivity was removed, and the cells were rinsed 2 times with PBS and then solubilized in 135 μL of NaOH (100 mmol/L). The solubilized cells were transferred to γ-counting tubes and the cell-bound radioactivity measured in a γ-counter. The B_{max} values were calculated by fitting a plot of cell-bound ^{111}In-pertuzumab (nanomoles) versus the concentration of unbound radioligand (nanomoles per liter) to a 1-site saturation binding model using Prism software. B_{max} values (nanomole) were converted to the number of *HER2* receptors per cell by counting the number of cells from control plates that were similarly seeded, treated with trastuzumab, and identically handled. Each assay was performed in duplicate and repeated in 3–6 separate experiments. Results are shown as the mean ± SD for all experiments.

Flow Cytometry and Confocal Microscopic Analysis of HER2 Density

For flow cytometry, cells were seeded into T75 flasks (Sarstedt) and cultured overnight. They were then exposed to trastuzumab (14 μg/mL) in culture medium or to PBS in medium (control) for 72 h at 37°C. The cells were rinsed twice with cold PBS and harvested. Fluorescein isothiocyanate (FITC)–conjugated anti-*HER2/neu* IgG$_1$ (20 μL, Clone Neu 24.7; BD Biosciences), which binds to a different epitope from trastuzumab, was incubated for 45 min at 4°C with 80 μL of a suspension of 1.3×10^7 cells/mL in ice-cold Ca^{2+}- and Mg^{2+}-free PBS (BD Biosciences) containing 0.2% bovine serum albumin and 0.1% NaN_3. Cells were recovered by centrifugation at 250*g* for 5 min, rinsed twice with 1 mL of cold PBS, and resuspended in 200 μL of 4% formaldehyde in PBS. Flow

cytometry was performed using a FACScan (BD Biosciences), with 10,000 events recorded. Negative controls (no immunofluorescence staining) and isotype controls (FITC-mouse IgG$_1$; eBioscience) were included. No nonspecific binding was observed for the different cell lines or treatment conditions. Datasets were analyzed using CELLQuest software (version 3.3; BD Biosciences). Results were reported as the mean fluorescence intensity (MFI) calculated by subtracting the fluorescence intensity of the negative control from the fluorescence of cells stained for *HER2/neu*.

For confocal microscopy, $4-6 \times 10^5$ SKBr-3, MDA-MB-361, or MDA-MB-231 cells were seeded into chamber slides (Thermo Fisher Scientific) and cultured overnight. The medium was removed and the cells incubated with trastuzumab (14 µg/mL) in 400 µL of fresh medium for 72 h at 37°C. Cells were rinsed 3 times with PBS, and nonspecific binding sites were blocked for 2 h with 3% bovine serum albumin in Ca^{2+}- and Mg^{2+}-free PBS. Cells were rinsed once again with PBS and then incubated with FITC-anti-HER2/*neu* IgG$_1$ (BD Bioscience) for 1 h at RT. After 3 rinses with PBS, the cells were fixed with 3.7% paraformaldehyde for 30 min. The slides were mounted in Vectashield containing 4,6-diamidino-2-phenylindole (DAPI) (Vector Laboratories) and kept at 4°C overnight. Images were taken with an inverted LSM510 confocal microscope (Carl Zeiss) at the Advanced Optical Microscopy Facility (Princess Margaret Hospital). Excitation was at 364 and 490 nm for visualization of DAPI and FITC, using 385- to 470-nm and 525-nm emission filters, respectively. Images were analyzed using LSM-Viewer software (version 3.5.0.376; Carl Zeiss).

Effect of Trastuzumab on Binding of ^{111}In-DTPA-Pertuzumab In Vivo

Female athymic CD1 *nu/nu* mice (Charles River) were implanted with a 0.72-mg, 60-d sustained release 17β-estradiol pellet (Innovative Research of America). At least 24 h later, mice were inoculated subcutaneously with 1×10^7 MDA-MB-361 cells in 200 µL of a 1:1 mixture of Matrigel (BD Biosciences) and serum-free medium. After 2 wk, groups of 3–4 mice with 70 ± 10 mm^3 tumors (measured with external calipers and calculated using length × width$^2 \times 0.5$) were treated with trastuzumab (4 mg/kg) or nonspecific human IgG (hIgG, 4 mg/kg; product I4506 [Sigma-Aldrich]) or with an equivalent volume of PBS by intraperitoneal injection for 3 d. In a second study, groups of 3–4 tumor-bearing mice were treated with trastuzumab (4 mg/kg), hIgG (4 mg/kg), anti-CD20 mAb, rituximab (4 mg/kg), or an equivalent volume of PBS and then 2 mg/kg weekly for 2 wk. After the 3-d or 3-wk treatment courses, hIgG- and rituximab-treated mice were injected in the lateral tail vein with ^{111}In-DTPA-pertuzumab (10 µg; 0.04–0.05 MBq/µg) in 200 µL of sodium chloride injection USP. For trastuzumab- and PBS-treated mice, biodistribution studies were performed immediately after micro-SPECT/CT at 72 h after injection of ^{111}In-DTPA-pertuzumab (10 µg; 1.3–3.1 MBq/µg). A group of 4 mice received a 100-fold excess of unlabeled pertuzumab 24 h before injection of ^{111}In-DTPA-pertuzumab to evaluate the specificity of tumor uptake. At 72 after injection of ^{111}In-DTPA-pertuzumab, mice were sacrificed; tumor, blood, and normal tissues were then collected and weighed, and their radioactivity measured in a γ-counter. Tumor and normal-tissue uptake were expressed as mean $\pm$ SD percentage injected dose (%ID) per gram and as tumor-to-blood (T/B) and tumor-to-normal tissue (T/NT) ratios. The principles of laboratory animal care (NIH publication no. 86-23, revised 1985) were followed, and all animal studies were conducted under a protocol (no. 989.5) approved by the Animal

Care Committee at the University Health Network in accordance with Canadian Council on Animal Care guidelines.

Micro-SPECT/CT of Tumor HER2 Expression

Micro-SPECT/CT was performed at 72 h after the injection of ^{111}In-DTPA-pertuzumab (10 µg; 1.3–3.1 MBq/µg). Mice were anesthetized by inhalation of 2% isoflurane in O$_2$. Imaging was performed on a NanoSPECT/CT tomograph (Bioscan) equipped with 4 NaI detectors and fitted with 1.4-mm multipinhole collimators (full width at half maximum ≤ 1.2 mm). A total of 24 projections were acquired in a 256×256 acquisition matrix with a minimum of 80,000 counts per projection. Images were reconstructed using an ordered-subset expectation maximization algorithm (9 iterations). Quantification was performed by volume-of-interest (VOI) analysis using InvivoScope software (version 1.34beta6; Bioscan), and tumor and normal-tissue uptake were expressed as mean $\pm$ SD %ID per voxel (1 voxel, 0.008 mm^3). Cone-beam CT images were acquired (180 projections, 1 s/projection, 45 kVp) before micro-SPECT images. Coregistration of micro-SPECT and CT images was performed using InvivoScope software.

Immunohistochemical Staining of Explanted MDA-MB-361 Tumors

Excised tumors were cut into 2- to 3-mm sections, fixed in 10% neutral buffered formalin, and embedded in paraffin. Sections (4 µm thick) were dewaxed and rehydrated. Endogenous peroxidase and biotin activities were blocked using 3% H$_2$O$_2$ and an avidin and biotin blocking kit (Vector Laboratories), respectively. Sections were then blocked for 15 min with 10% normal serum and incubated with a mouse anti-c-erbB-2 monoclonal antibody (CB11; Novocastra Laboratories) at a 1:100 dilution for 1 h, followed by an antimouse biotinylated secondary antibody (Vector Laboratories) for 30 min and a horseradish peroxidase–conjugated ultrastreptavidin labeling reagent (ID Labs Inc.) for 30 min at RT. After the reaction product was rinsed twice with PBS, it was visualized using NovaRed solution (Vector Laboratories) and counterstained lightly with Mayer's hemotoxylin. Sections were then dehydrated, cleared in xylene, and mounted in Permount (Fisher Scientific). Negative control slides were prepared with omission of the primary anti-c-erbB-2 antibody. All samples were scored in a masked manner by a pathologist as the percentage of strong, complete, homogeneous membrane staining.

Statistical Analysis

Comparisons of the specific binding of ^{111}In-DTPA-pertuzumab to trastuzumab-exposed or control cells were made using a ratio *t* test ($P < 0.05$). Tumor uptake of ^{111}In-DTPA-pertuzumab in vivo was compared for different treatment groups by 1-way parametric ANOVA using the Bonferroni adjustment for multiple comparisons ($P < 0.05$). Correlations between biodistribution and imaging results were made using a Pearson correlation test ($P < 0.05$). All other statistical comparisons were made using a Student *t* test ($P < 0.05$).

RESULTS

^{111}In-DTPA-Pertuzumab

Pertuzumab was substituted with 1.4 ± 0.3 DTPA molecules per IgG and labeled with ^{111}In to a final RCP greater than 97%. SE-HPLC analysis showed 1 major peak (retention time [t_R] = 7.7 min) corresponding to ^{111}In-pertuzumab. The presence of aggregates or a higher-molecular-weight species was less than 10% ($t_R = 6.9$ min). The presence of

low-molecular-weight species, such as DTPA, was less than 1.5% (t_R = 13.0 min). ^{111}In-DTPA-pertuzumab demonstrated saturable binding to SKBr-3 cells with K_d and B_{max} values of 2.0 ± 1.0 nmol/L and 1.2 ± 0.2 × 10^6 receptors per cell, respectively; these were comparable to values previously reported for SK-OV-3 cells (15).

Competition for HER2 Binding on Breast Cancer Cells

^{111}In-DTPA-pertuzumab binding to SKBr-3 or MDA-MB-361 cells was not displaced by increasing concentrations of trastuzumab up to 500 nmol/L, indicating that trastuzumab does not interfere with ^{111}In-DTPA-pertuzumab binding to its epitope on *HER2* (Fig. 1). The proportion of cell-bound radioactivity was greater for SKBr-3 cells than for MDA-MB-361 cells because of their greater *HER2* expression (7).

Effect of Trastuzumab on Binding of ^{111}In-DTPA-Pertuzumab In Vitro

The saturation binding of ^{111}In-DTPA-pertuzumab by SKBr-3 cells exposed to trastuzumab (14 μg/mL) at 37°C was significantly reduced to 82% ± 6% ($P = 0.0094$), 70% ± 10% ($P = 0.012$), and 62% ± 2% ($P = 0.0001$), compared with untreated cells at 24, 48, and 72 h, respectively (Fig. 2A and Supplemental Fig. 1; supplemental materials are available online only at http://jnm.snmjournals.org). Higher or lower concentrations of trastuzumab (1, 3, 7, or 56 μg/mL), compared with 14 μg/mL, did not result in increased or decreased ^{111}In-DTPA-pertuzumab binding ($P = 0.68$, data not shown). The effects of trastuzumab on binding of ^{111}In-DTPA-pertuzumab were more profound for MDA-MB-361 than for SKBr-3 cells. Exposure to trastuzumab (14 μg/mL) for 24, 48, or 72 h significantly reduced binding to 31% ± 13% ($P = 0.0012$), 32% ± 13% ($P = 0.0009$), and 32% ± 9% ($P = 0.0002$), respectively, compared with control untreated cells (Fig. 2B and Supplemental Fig. 1). Rituximab or hIgG (14 μg/mL) did not significantly reduce ^{111}In-DTPA-

FIGURE 2. Binding of ^{111}In-DTPA-pertuzumab to SKBr-3 (A) and MDA-MB-361 (B) human breast cancer cells at selected times after incubation with trastuzumab, rituximab, or nonspecific hIgG (14 μg/mL). Values shown represent mean ± SD of repeated experiments (n = 3–6). Statistically significant differences, compared with unexposed cells, are shown (*$P < 0.05$, **$P < 0.01$, ***$P < 0.001$).

pertuzumab binding at 24, 48, or 72 h, compared with untreated cells ($P = 0.13$–0.96; Figs. 2A and 2B).

Flow Cytometry and Confocal Microscopic Analysis of HER2 Density

Flow cytometry and confocal microscopy showed that MDA-MB-231 cells with low *HER2* density exposed to PBS or trastuzumab (14 μg/mL) for 72 h at 37°C did not significantly bind FITC-conjugated anti-*HER2/neu* IgG$_1$ antibodies (MFI, 2.8 vs. 2.0, respectively; Fig. 3A). In contrast, MDA-MB-361 and SKBr-3 cells with intermediate or high *HER2* expression exposed to trastuzumab exhibited a 60% and 39% reduction, respectively, in their binding of anti-*HER2/neu* antibodies, compared with PBS-treated cells (MFI, 26.2 vs. 66.2 and 66.0 vs. 107.4, respectively; Figs. 3B and 3C). Confocal microscopy of MDA-MB-361 or SKBr-3 cells exposed to PBS showed moderate or high *HER2* membrane staining, respectively (Figs. 3B and 3C). Exposure to trastuzumab markedly reduced membrane staining for *HER2*, especially for MDA-MB-361 but also for SKBr-3 cells.

Effect of Trastuzumab on Binding of ^{111}In-DTPA-Pertuzumab In Vivo

The tumor and normal-tissue uptake of ^{111}In-DTPA-pertuzumab and T/NT ratios at 72 h after injection in athymic
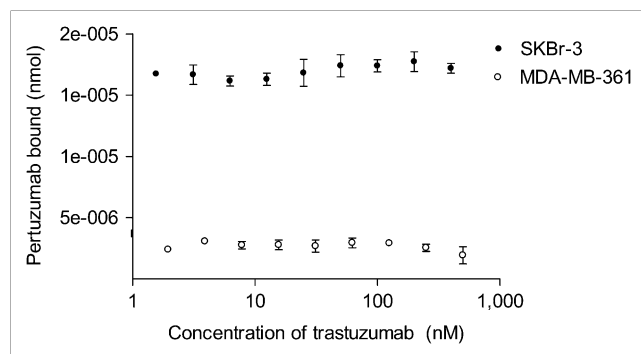

FIGURE 1. Displacement of binding of ^{111}In-DTPA-pertuzumab in vitro to SKBr-3 or MDA-MB-361 cells by increasing concentrations of trastuzumab. Higher binding of ^{111}In-DTPA-pertuzumab to SKBr-3 cells, compared with MDA-MB-361 cells, is due to their greater *HER2* expression. Data are presented from 1 representative assay and points represent mean ± SD of duplicate determinations. Assay was repeated in 3 separate experiments.
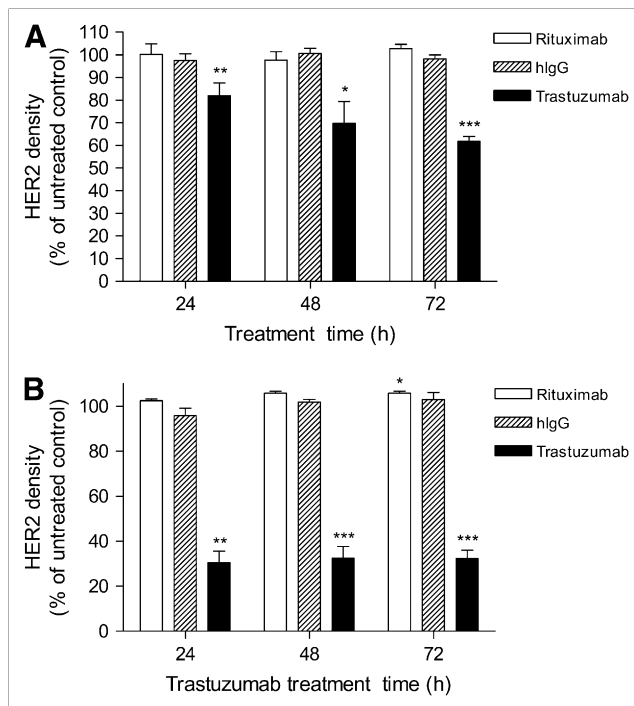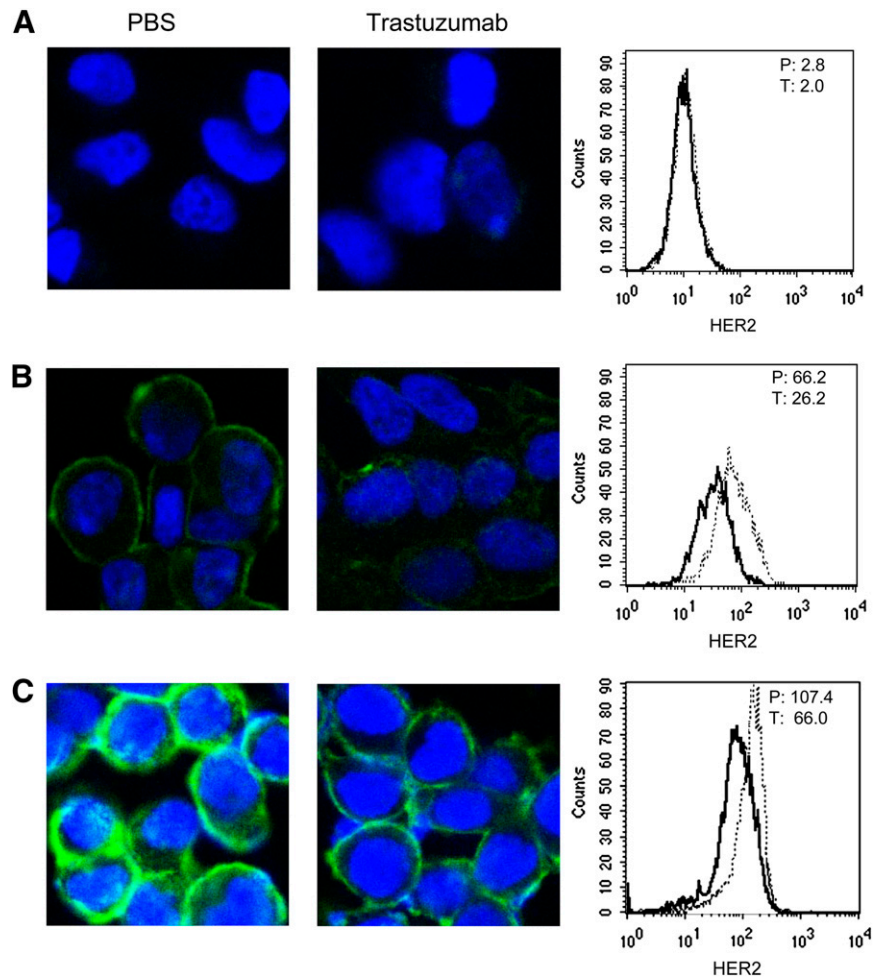
FIGURE 3. Confocal immunofluorescence microscopy (left and center) and flow cytometry (right) of MDA-MB-231 (A), MDA-MB-361 (B), and SKBr-3 (C) cells exposed to PBS (left) or trastuzumab (14 μg/mL) (center) for 72 h. HER2 was detected using FITC-conjugated anti-HER2/*neu* IgG$_1$ (green), and nucleus was counterstained with DAPI. For flow cytometry, MFI of trastuzumab-treated (T; bold line) and PBS-treated (P; dashed line) cells is indicated in top right corner.

mice bearing MDA-MB-361 xenografts is shown in Table 1. There was high tumor accumulation of radioactivity (34.6 ± 9.9 %ID/g), with a T/B ratio of 5.9 ± 1.4. Preinjection of a 100-fold excess of unlabeled pertuzumab (1 mg) 24 h before ^{111}In-DTPA-pertuzumab decreased tumor uptake 4.4-fold (7.8 ± 0.5 %ID/g vs. 34.6 ± 9.9 %ID/g, respectively; $P <$ 0.01) and reduced the T/B ratio to 1.4 ± 0.3 ($P <$ 0.01), demonstrating that accumulation was *HER2*-specific. The highest normal-tissue uptake of radioactivity was found in the kidneys, liver, and spleen; these concentrations were similar to those previously reported for ^{111}In-DTPA-trastuzumab (7). T/NT ratios were highest for muscle and lowest for the kidneys (Table 1).

Tumor uptake of ^{111}In-DTPA-pertuzumab at 72 h after injection was more than 2-fold lower in mice treated with trastuzumab (4 mg/kg) for 3 d than in mice receiving PBS (13.5 ± 2.6 %ID/g vs. 28.5 ± 9.1 %ID/g, $P <$ 0.05; Fig. 4A and Supplemental Table 1). There also appeared to be decreased tumor accumulation of ^{111}In-DTPA-pertuzumab in mice treated with hIgG, compared with PBS-treated mice, but this was not statistically significant (21.8 ± 1.1 %ID/g vs. 28.5 ± 9.1 %ID/g, $P >$ 0.05). A second study was performed to evaluate the ability of ^{111}In-DTPA-pertuzumab to detect a therapeutic response to trastuzumab when administered at 4

mg/kg followed by weekly doses of 2 mg/kg for 2 wk. Tumor accumulation of ^{111}In-DTPA-pertuzumab was 4.5-fold lower in trastuzumab-treated mice than in those treated with PBS (7.6 ± 0.4 %ID/g vs. 34.6 ± 9.9 %ID/g, $P <$ 0.001; Fig. 4B and Supplemental Table 1). Again, tumor uptake of ^{111}In-DTPA-pertuzumab was not significantly diminished in mice treated with hIgG or rituximab, compared with mice treated with PBS (25.0 ± 2.1 %ID/g and 23.2 ± 5.3 %ID/g, respectively; $P >$ 0.05).

Micro-SPECT/CT of Tumor HER2 Expression

Micro-SPECT/CT images of athymic mice bearing MDA-MB-361 tumors treated with PBS at 72 h after injection of ^{111}In-DTPA-pertuzumab revealed strong tumor uptake; treatment with trastuzumab (4 mg/kg) for 3 d, however, diminished uptake considerably (Figs. 5A and 5B). VOI analysis revealed a 2-fold reduction in tumor radioactivity, compared with PBS-treated mice (4.9 ± 1.2 × 10^{-5} %ID/voxel vs. 1.0 ± 0.35 × 10^{-4} %ID/voxel, $P = 0.05$; Fig. 5E). Mice receiving PBS for 3 wk showed strong tumor uptake, but this was dramatically diminished in mice treated with trastuzumab (4 mg/kg, followed by 2 mg/kg weekly; Figs. 5C and 5D). Because of poor tumor signal, VOI analysis could not be reliably performed on mice treated with trastuzumab

TABLE 1. Tumor and Normal-Tissue Distribution of Radioactivity in Athymic Mice Implanted Subcutaneously with MDA-MB-361 Human Breast Cancer Xenografts at 72 h After Injection of ^{111}In-DTPA-Pertuzumab

	Not blocked		Blocked	
Site	%ID/g	T/NT	%ID/g	T/NT
Blood	5.9 ± 0.4	5.9 ± 1.4	5.6 ± 0.7	1.4 ± 0.3
Heart	1.7 ± 0.2	20.7 ± 6.4	1.8 ± 0.2	4.5 ± 0.8
Lungs	3.5 ± 0.4	9.5 ± 2.4	3.1 ± 0.6	2.6 ± 0.6
Liver	8.5 ± 1.2	4.1 ± 1.6	8.4 ± 1.1	0.9 ± 0.2
Spleen	7.8 ± 2.0	4.4 ± 1.3	5.2 ± 0.6	1.5 ± 0.3
Kidneys	15.3 ± 0.4	2.3 ± 0.6	12.8 ± 1.9	0.6 ± 0.0
Small intestine	2.0 ± 0.3	18.1 ± 6.4	2.0 ± 0.1	3.9 ± 0.5
Large intestine	1.5 ± 0.1	22.8 ± 7.5	1.1 ± 0.0	6.8 ± 0.5
Muscle	0.9 ± 0.1	37.9 ± 9.5	0.9 ± 0.1	8.8 ± 0.1
Tumor	34.6 ± 9.9*	1.0 ± 0.0	7.8 ± 0.5	1.0 ± 0.0

*Statistically significant difference ($P < 0.01$), compared with blocked group.

Groups of 3–4 tumor-bearing athymic mice were injected intravenously with ^{111}In-DTPA-pertuzumab (10 µg) without (not blocked) or with (blocked) preinjection of 1 mg of unlabeled pertuzumab.

for 3 wk. There was a strong linear correlation between tumor VOI and biodistribution results ($r = 0.97$, $P < 0.0005$).

Immunohistochemical Staining of Explanted Tumors

HER2 downregulation was not apparent in explanted MDA-MB-361 tumors stained immunohistochemically with *HER2/neu* antibodies from mice treated with trastuzumab (4 mg/kg) for 3 d, compared with mice treated with PBS (Fig. 6 and Supplemental Table 2). Hematoxylin and eosin staining identified these sections as containing malignant cells. Explanted MDA-MB-361 tumors from mice treated for 3 wk
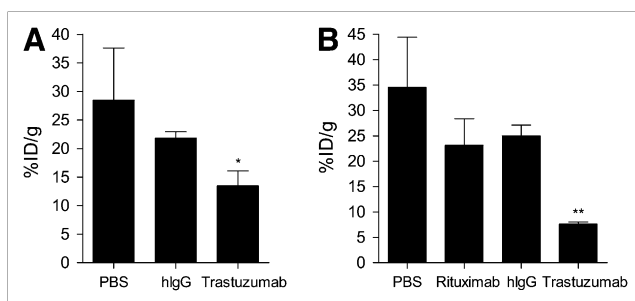

FIGURE 4. Tumor uptake of ^{111}In-DTPA-pertuzumab at 72 h after injection in athymic mice bearing subcutaneous MDA-MB-361 xenografts at 3 d after treatment with PBS or 4 mg of nonspecific human IgG (hIgG) or trastuzumab per kilogram (A) or 3 wk after treatment with PBS, rituximab, hIgG, or trastuzumab (loading dose of 4 mg/kg followed by weekly doses of 2 mg/kg) (B). Significant differences, compared with PBS-treated mice, are shown (*$P < 0.05$, **$P < 0.001$). Values shown represent mean ± SD of replicate determinations ($n = 3–4$).

resulted in the elimination of *HER2* immunopositivity; this was associated with almost complete eradication of viable tumor cells (Fig. 6 and Supplemental Table 2).

DISCUSSION

In this study, we showed for the first time, to our knowledge, that micro-SPECT/CT with ^{111}In-DTPA-pertuzumab sensitively detected changes in the concentration of *HER2* in tumor tissue in subcutaneous BC xenografts in athymic mice caused by trastuzumab (Herceptin). Pertuzumab is a promising new immunotherapeutic agent for *HER2*-expressing BC, which aims to prevent dimerization with other HER family members; such dimerization is responsible for potent mitogenic signaling (*16*). Only 1 other group has reported the tumor and normal-tissue distribution of pertuzumab, in this case ^{177}Lu-pertuzumab in athymic mice bearing subcutaneous *HER2*-positive SK-OV-3 human ovarian cancer xenografts (*15*). In this earlier study, lower kidney, liver, and spleen uptake was observed with ^{177}Lu-pertuzumab than with ^{111}In-DTPA-pertuzumab, possibly because of the higher in vivo stability of the radiometal complexed to the isothiocyanate-benzyl-CHX-A″-DTPA used.

A 2-fold decreased tumor uptake of ^{111}In-DTPA-pertuzumab was measured in mice bearing MDA-MB-361 xenografts treated with trastuzumab (4 mg/kg) for 3 d, compared with PBS-treated controls (Fig. 4A). Decreased tumor radioactivity was also visualized by micro-SPECT/CT and quantified by VOI image analysis (Figs. 5A, 5B, and 5E). These findings indicate an early effect of trastuzumab in promoting *HER2* downregulation rather than reducing the number of viable *HER2*-positive tumor cells over this short time. MDA-MB-361 cells exposed in vitro to trastuzumab (14 µg/mL) for only 24 h similarly exhibited a 70% reduction in the binding of ^{111}In-DTPA-pertuzumab, compared with untreated cells (Fig. 2B). Interestingly, this same concentration of trastuzumab (14 µg/mL) only decreased the binding of ^{111}In-DTPA-pertuzumab to SKBr-3 cells by a maximum of 38% at 72 h (Fig. 2A). It was not possible to evaluate the effect of treatment with trastuzumab in vivo on the uptake of ^{111}In-DTPA-pertuzumab in SKBr-3 cells, because these cells are poorly tumorigenic in athymic mice. The differences between MDA-MB-361 and SKBr-3 cells in *HER2* downregulation caused by trastuzumab are consistent with earlier reports that *HER2* on SKBr-3 cells are internalization-impaired (*17,18*). Hashizume et al. (*17*) proposed that coexistent *HER3* on SKBr-3 cells may impair *HER2* internalization; however, in our study, radioligand binding assays with ^{111}In-DTPA-pertuzumab and flow cytometry and immunofluorescence confocal microscopy demonstrated that *HER2* on MDA-MB-361 cells was downregulated by trastuzumab, despite the fact that these cells have *HER3* expression similar to that of SKBr-3 cells (*19*). Interestingly, although hIgG and rituximab caused no changes in *HER2* expression levels in SKBr-3 and MDA-MB-361 cells in vitro, there was an apparent but statistically insignificant decrease in tumor uptake of [111]In-
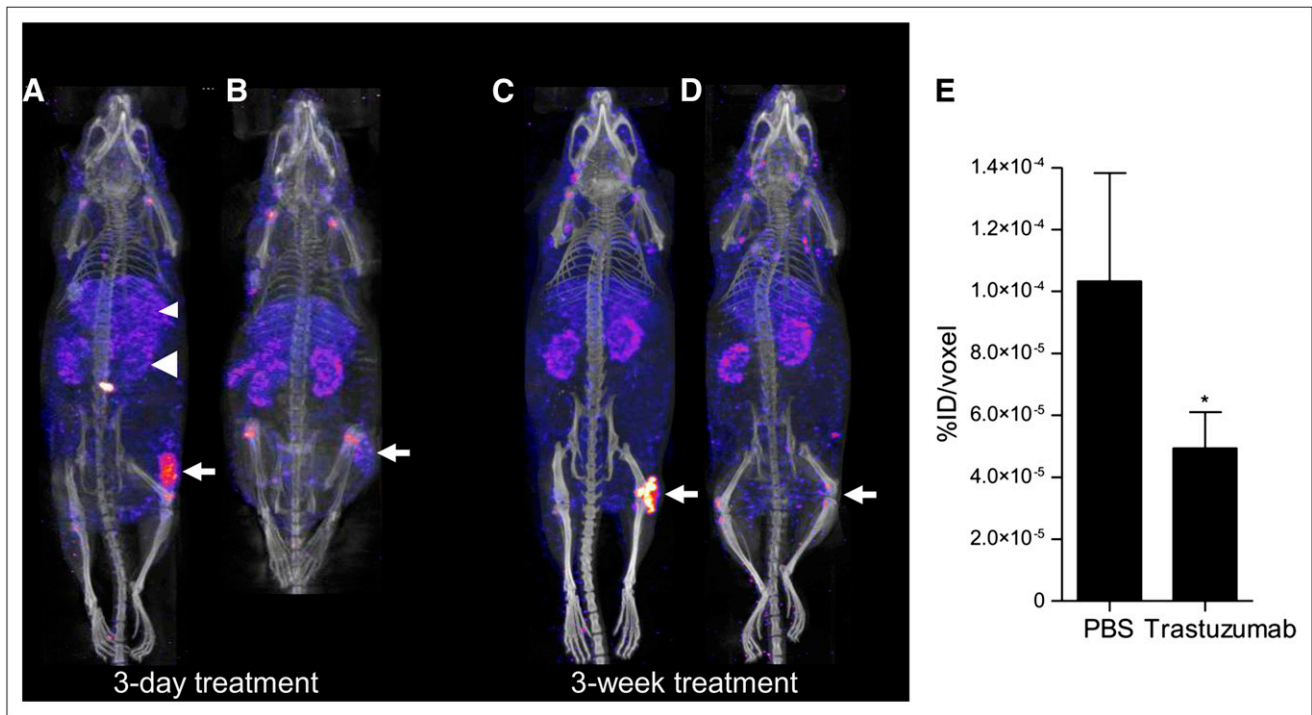
FIGURE 5. Posterior whole-body micro-SPECT/CT images of representative athymic mice implanted subcutaneously in the right hind leg with MDA-MB-361 human BC xenografts (white arrow) at 72 h after injection of ^{111}In-DTPA-pertuzumab. Mice were treated for 3 d with PBS (A) or 4 mg/kg of trastuzumab (B) or for 3 wk with PBS (C) or 4 mg/kg, followed by 2 weekly doses of trastuzumab (2 mg/kg) (D). Also visualized are liver (small arrowhead) and kidneys (large arrowhead). There is small superficial laceration on back of mouse in A that nonspecifically accumulated radioactivity. VOI analysis (E) of images in A and B showed 52% decrease in tumor radioactivity after treatment with trastuzumab (*$P = 0.05$). VOI analysis was not performed in D because of the inability to clearly delineate tumors in trastuzumab-treated mice.

DTPA-pertuzumab mice treated with hIgG or rituximab in vivo. The reason for this phenomenon is not known.

HER2 downregulation is proposed as one means by which trastuzumab exerts its antitumor effects, but the relationship between tumor response in patients to the drug and its ability
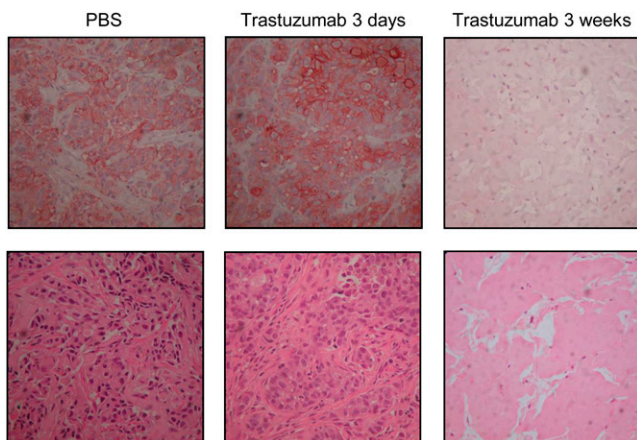

FIGURE 6. Immunohistochemical staining (upper row) using CB11 anti-*HER2/neu* antibodies of explanted representative MDA-MB-361 xenografts treated with PBS or trastuzumab for 3 d or 3 wk. Bottom row shows hematoxylin and eosin staining of immunostained sections.

to diminish *HER2* density is not proven (*13*). Trastuzumab-mediated *HER2* downregulation has been reported in human BC cells in vitro (*20–22*) and in BC xenografts in mice in vivo (*23,24*). However, Austin et al. (*25*) proposed that in SKBr-3 and BT-474 cells, there is continual recycling of *HER2* from the cell surface to endosomes and back and that *HER2*-bound trastuzumab accompanies these recycling receptors but does not promote *HER2* downregulation. A pilot clinical study aimed at identifying the mechanisms of action of trastuzumab in patients who were receiving the drug preoperatively found no significant change in tumor *HER2* expression evaluated by immunohistochemical staining after treatment with 4 mg/kg, followed by 3 weekly doses of 2 mg/kg (*26*). Others have reported changes in *HER2* status only in small subsets of patients treated with trastuzumab (*27,28*).

Possible explanations for these differing conclusions regarding trastuzumab-mediated *HER2* downregulation are variability in receptor downregulation between tumors in different patients or among different cell lines (as shown for SKBr-3 and MDA-MB-361 cells; Fig. 2) and insensitivity in immunohistochemical staining for the detection of changes in *HER2* density, particularly when *HER2* is heterogeneously downregulated within a lesion. *HER2* 3+ positivity is defined as uniform, intense membrane staining of greater than 30% of tumor cells in a BC specimen (*4*). Thus, *HER2* downregulation

could occur in up to 70% of tumor cells and yet the specimen would still be designated as *HER2* 3+. In our study, there was significantly decreased uptake of ^{111}In-DTPA-pertuzumab in MDA-MB-361 xenografts in mice treated with trastuzumab for 3 d (Figs. 4A, 5A, and 5B) but no apparent decrease in *HER2* positivity by immunohistochemical staining (Fig. 6). Kramer-Marek et al. also recently showed that immunohistochemical staining was insensitive to changes ($\leq$70% reduction) in *HER2* density of BT-474 BC xenografts in athymic mice caused by treatment with the heat shock protein-90 (Hsp90) inhibitor 17-demethoxygeldanamycin (17-DMAG) (*29*). However, a 3-fold decreased tumor uptake of ^{18}F-labeled *HER2* affibody was found by small-animal PET and biodistribution studies. Moreover, decreased *HER2* was confirmed ex vivo by Western blot and enzyme-linked immunosorbent assay.

Smith-Jones et al. were the first to show that PET with ^{68}Ga-labeled trastuzumab F(ab$'$)$_2$ fragments could detect a 50% decrease in *HER2* density in BT-474 xenografts in mice caused by treatment with the Hsp90 inhibitor 17-allylaminogeldamycin (*11*). Nonetheless, radiolabeled trastuzumab and its fragments are not optimal for imaging trastuzumab-mediated *HER2* downregulation because they bind to the same epitope and thus are not able to differentiate between *HER2* blocking by trastuzumab and receptor downregulation. Antibody probes such as ^{111}In-DTPA-pertuzumab or Affibodies (*9,29*) that recognize epitopes on *HER2* unique from that of trastuzumab can be used to differentiate these 2 processes. The faster blood clearance and higher T/B ratios of Affibodies, antibody fragments, or engineered antibody constructs may offer advantages over pertuzumab for imaging *HER2* downregulation, especially in the clinical setting in which same-day imaging may be achieved.

We also examined the tumor uptake of ^{111}In-DTPA-pertuzumab at 72 h after injection in athymic mice bearing MDA-MB-361 xenografts treated for 3 wk with trastuzumab. In these studies, there was a 4.5-fold decrease in ^{111}In-DTPA-pertuzumab uptake in MDA-MB-361 xenografts measured in biodistribution studies, compared with mice treated with PBS ($P < 0.001$). Micro-SPECT/CT clearly identified tumors in the control mice receiving PBS, but tumors in trastuzumab-treated mice were not visualized (Figs. 5C and 5D). Immunohistochemical examination of the explanted tumors in trastuzumab-treated mice revealed a dramatic decrease in viable and *HER2*-positive tumor cells, compared with PBS-treated mice (Fig. 6). In contrast, there was no apparent decrease in viable tumor cells in mice treated with trastuzumab for only 3 d, compared with PBS-treated controls (Fig. 6). In patients, the assessment of tumor viability changes for correlation with the uptake of ^{111}In-DTPA-pertuzumab could potentially be assessed by PET using ^{18}F-FDG without the need for tissue sampling (*30*). Overall, our results demonstrated that micro-SPECT/CT with ^{111}In-DTPA-pertuzumab was powerful in its ability to detect a tumor response to trastuzumab over a longer time while visualizing an early molecular response (i.e., *HER2* downregulation) shortly after starting treatment with the drug.

CONCLUSION

Micro-SPECT/CT with ^{111}In-DTPA-pertuzumab in athymic mice bearing subcutaneous MDA-MB-361 BC xenografts sensitively detected tumor *HER2* downregulation associated with an early molecular response to trastuzumab and a longer-term tumor response due to eradication of viable *HER2*-positive BC cells. Immunohistochemical staining of explanted tumors was insufficiently sensitive to detect trastuzumab-mediated decreases in *HER2* density. ^{111}In-DTPA-pertuzumab may be valuable for imaging molecular and tumor response to trastuzumab in BC patients.

REFERENCES

1. McLarty K, Reilly R. Molecular imaging as a tool for targeted and personalized cancer therapy. *Clin Pharmacol Ther.* 2007;81:420–424.
2. Hudis C. Trastuzumab: mechanism of action and use in clinical practice. *N Engl J Med.* 2007;357:39–51.
3. Viani G, Afonso S, Stefano E, De Fendi L, Soares F. Adjuvant trastuzumab in the treatment of her-2-positive early breast cancer: a meta-analysis of published randomized trials. *BMC Cancer.* 2007;7:153–163.
4. Wolff A, Hammond M, Schwartz J, et al. American Society of Clinical Oncology/ College of American Pathologists guideline recommendations for human epidermal growth factor receptor 2 testing in breast cancer. *J Clin Oncol.* 2007;25:118–145.
5. Slamon D, Leyland-Jones B, Shak S, et al. Use of chemotherapy plus a monoclonal antibody against HER2 for metastatic breast cancer that overexpresses HER2. *N Engl J Med.* 2001;344:783–792.
6. Adams G, Schier R, Marshall K, et al. Increased affinity leads to improved selective tumor delivery of single-chain Fv antibodies. *Cancer Res.* 1998;58:485–490.
7. McLarty K, Cornelissen B, Scollard D, Done S, Chun K, Reilly R. Associations between the uptake of ^{111}In-DTPA-trastuzumab, HER2 density and response to trastuzumab (Herceptin) in athymic mice bearing subcutaneous human tumour xenografts. *Eur J Nucl Med Mol Imaging.* 2009;36:81–93.
8. Olafsen T, Tan G, Cheung C, et al. Characterization of engineered anti-p185[HER-2] (scFv-C$_H$3)$_2$ antibody fragments (minibodies) for tumor targeting. *Protein Eng Des Sel.* 2004;17:315–323.
9. Orlova A, Tran T, Widström C, Engfeldt T, Eriksson Karlström A, Tolmachev V. Pre-clinical evaluation of [^{111}In]-benzyl-DOTA-Z$_{HER2:342}$, a potential agent for imaging of HER2 expression in malignant tumors. *Int J Mol Med.* 2007;20:397–404.
10. Robinson M, Doss M, Shaller C, et al. Quantitative immuno-positron emission tomography imaging of HER2-positive tumor xenografts with an iodine-124 labeled anti-HER2 diabody. *Cancer Res.* 2005;65:1471–1478.
11. Smith-Jones P, Solit D, Akhurst T, Afroze F, Rosen N, Larson S. Imaging the pharmacodynamics of HER2 degradation in response to Hsp90 inhibitors. *Nat Biotechnol.* 2004;22:701–706.
12. Tang Y, Wang J, Scollard D, et al. Imaging of HER2/neu-positive BT-474 human breast cancer xenografts in athymic mice using ^{111}In-trastuzumab (Herceptin) Fab fragments. *Nucl Med Biol.* 2005;32:51–58.
13. Valabrega G, Montemurro F, Aglietta M. Trastuzumab: mechanism of action, resistance and future perspectives in HER2-overexpressing breast cancer. *Ann Oncol.* 2007;18:977–984.
14. Albanell J, Codony J, Rovira A, Mellado B, Gascon P. Mechanism of action of anti-HER2 monoclonal antibodies: scientific update on trastuzumab and 2C4. *Adv Exp Med Biol.* 2003;532:253–268.
15. Persson M, Tolmachev V, Andersson K, Gedda L, Sandstrom M, Carlsson J. [^{177}Lu]pertuzumab: experimental studies on targeting of HER-2 positive tumour cells. *Eur J Nucl Med Mol Imaging.* 2005;32:1457–1462.
16. Badache A, Hynes NE. A new therapeutic antibody masks ErbB2 to its partners. *Cancer Cell.* 2004;5:299–301.

17. Hashizume T, Fukuda T, Nagaoka T, et al. Cell type dependent endocytic internalization of ErbB2 with an artificial peptide ligand that binds to ErbB2. *Cell Biol Int.* 2008;32:814–826.

18. Hommelgaard AM, Lerdrup M, van Deurs B. Association with membrane protrusions makes ErbB2 an internalization-resistant receptor. *Mol Biol Cell.* 2004;15:1557–1567.

19. Folgiero V, Avetrani P, Bon G, et al. Induction of ErbB-3 expression by $\alpha_6\beta_4$ integrin contributes to tamoxifen resistance in ERβ1-negative breast carcinomas. *PLoS One.* 2008;3:e1592.

20. Cuello M, Ettenberg SA, Clark AS, et al. Down-regulation of the erbB-2 receptor by trastuzumab (herceptin) enhances tumor necrosis factor-related apoptosis-inducing ligand-mediated apoptosis in breast and ovarian cancer cell lines that overexpress erbB-2. *Cancer Res.* 2001;61:4892–4900.

21. Hudziak RM, Lewis GD, Winget M, Fendly BM, Shepard HM, Ullrich A. p185[HER2] monoclonal antibody has antiproliferative effects in vitro and sensitizes human breast tumor cells to tumor necrosis factor. *Mol Cell Biol.* 1989;9: 1165–1172.

22. Mittendorf EA, Storrer CE, Shriver CD, Ponniah S, Peoples GE. Investigating the combination of trastuzumab and HER2/neu peptide vaccines for the treatment of breast cancer. *Ann Surg Oncol.* 2006;13:1085–1098.

23. Lee S, Yang W, Lan KH, et al. Enhanced sensitization to taxol-induced apoptosis by herceptin pretreatment in ErbB2-overexpressing breast cancer cells. *Cancer Res.* 2002;62:5703–5710.

24. Warburton C, Dragowska WH, Gelmon K, et al. Treatment of HER-2/neu overexpressing breast cancer xenograft models with trastuzumab (Herceptin) and gefitinib (ZD1839): drug combination effects on tumor growth, HER-2/neu and epidermal growth factor receptor expression, and viable hypoxic cell fraction. *Clin Cancer Res.* 2004;10:2512–2524.

25. Austin CD, De Maziere AM, Pisacane PI, et al. Endocytosis and sorting of ErbB2 and the site of action of cancer therapeutics trastuzumab and geldanamycin. *Mol Biol Cell.* 2004;15:5268–5282.

26. Gennari R, Menard S, Fagnoni F, et al. Pilot study of the mechanism of action of preoperative trastuzumab in patients with primary operable breast tumors overexpressing HER2. *Clin Cancer Res.* 2004;10:5650–5655.

27. Burstein HJ, Harris LN, Gelman R, et al. Preoperative therapy with trastuzumab and paclitaxel followed by sequential adjuvant doxorubicin/cyclophosphamide for HER2 overexpressing stage II or III breast cancer: a pilot study. *J Clin Oncol.* 2003;21:46–53.

28. Harris LN, You F, Schnitt SJ, et al. Predictors of resistance to preoperative trastuzumab and vinorelbine for HER2-positive early breast cancer. *Clin Cancer Res.* 2007;13:1198–1207.

29. Kramer-Marek G, Kiesewetter D, Capala J. HER2 expression changes in breast cancer xenografts following therapeutic intervention can be quantified using PET imaging and ^{18}F-labelled affibody molecules. *J Nucl Med.* 2009;50:1131–1139.

30. Rosen E, Eubank W, Mankoff D. FDG PET, PET/CT, and breast cancer imaging. *Radiographics.* 2007;27(suppl 1):S215–S229.